

Multi-Objective Beamforming for Energy-Efficient SWIPT Systems

Shiyang Leng[§], Derrick Wing Kwan Ng^{*}, Nikola Zlatanov[†], and Robert Schober[‡]

The Pennsylvania State University, USA[§]

The University of New South Wales, Australia^{*}

Monash University, Australia[†]

Friedrich-Alexander-University Erlangen-Nürnberg (FAU), Germany[‡]

Abstract—In this paper, we study the resource allocation algorithm design for energy-efficient simultaneous wireless information and power transfer (SWIPT) systems. The considered system comprises a transmitter, an information receiver, and multiple energy harvesting receivers equipped with multiple antennas. We propose a multi-objective optimization framework to study the trade-off between the maximization of the energy efficiency of information transmission and the maximization of wireless power transfer efficiency. The proposed problem formulation takes into account the per antenna circuit power consumption of the transmitter and the imperfect channel state information of the energy harvesting receivers. The adopted non-convex multi-objective optimization problem is transformed into an equivalent rank-constrained semidefinite program (SDP) and optimally solved by SDP relaxation. Numerical results unveil an interesting trade-off between the considered conflicting system design objectives and reveal the benefits of multiple transmit antennas for improving system energy efficiency.

I. INTRODUCTION

In recent years, the development of wireless communication networks worldwide has triggered an exponential growth in the number of wireless devices and sensors for applications such as e-health and environmental monitoring. The related tremendous increase in the number of transmitter(s) and receiver(s) has also led to a huge demand for energy and a better energy management. Hence, energy efficient system designs, which adopt energy efficiency (bit-per-Joule) as the performance metric, have been recently proposed [1]–[4]. In [2], energy-efficient power allocation schemes were proposed for cognitive radio systems. In [3], energy-efficient link adaptation was investigated for the maximization of energy efficiency in frequency-selective channels. In [4], the authors proposed a resource allocation algorithm design for energy-efficient communication in multicarrier communication systems with hybrid energy harvesting base stations. Although energy-efficient resource allocation algorithm designs for traditional communication networks have been studied in the literature, mobile receivers are often powered by batteries with limited energy storage which remain the system performance bottlenecks in perpetuating the lifetime of wireless networks.

Energy harvesting (EH) based communication system design is a viable solution for prolonging the lifetime of energy-limited devices. Conventional natural sources, such as wind, solar, and biomass, have been exploited as energy sources

for fixed-location, outdoor transmitters. However, these natural energy sources are often location and weather dependent and may not be suitable for mobile receivers. On the other hand, wireless power transfer (WPT) via electromagnetic waves in radio frequency (RF) enables a comparatively controllable energy harvesting for mobile receivers. In fact, recent progress in the development of RF-EH circuitries has made RF-EH practical for low-power consumption devices [5]–[7], e.g. wireless sensors. Besides, WPT enables the dual use of the information carrier for simultaneous wireless information and power transfer (SWIPT) [8]–[10]. Different from traditional wireless communication systems, where data rate and energy efficiency are the most fundamental system performance metrics, in SWIPT systems, the wireless energy transfer efficiency is an equally important QoS metric. Thus, the design of resource allocation algorithms should take into account the emerging need for energy transfer efficiency. In [11], the authors studied the fundamental rate-energy trade-off region for optimal information beamforming. In [12], power allocation, user scheduling, and subcarrier allocation were jointly designed to enable an energy-efficient multicarrier SWIPT system. In [13], the authors proposed the use of large scale multiple-antenna systems for improving energy efficiency of SWIPT. Although energy-efficient data communication design and energy-efficient WPT have already been studied individually, the trade-off between these two system design paradigms is still unclear for SWIPT systems. In particular, these two design goals may conflict with each other but both are desirable to system designer. However, the single-objective resource allocation algorithms proposed in [2]–[4], [8]–[11], [13] may no longer be applicable in energy-efficient SWIPT networks.

In this paper, we address the above issues. To this end, we formulate the resource allocation algorithm design as a multi-objective optimization problem which strikes a balance between the maximization of energy efficiency of information transmission and the maximization of WPT efficiency. The resulting non-convex optimization problem is solved optimally by semidefinite programming (SDP) relaxation. Simulation results illustrate the trade-off between the conflicting system design objectives.

II. SYSTEM MODEL

In this section, we first define the adopted notations and then present the channel model for energy-efficient SWIPT

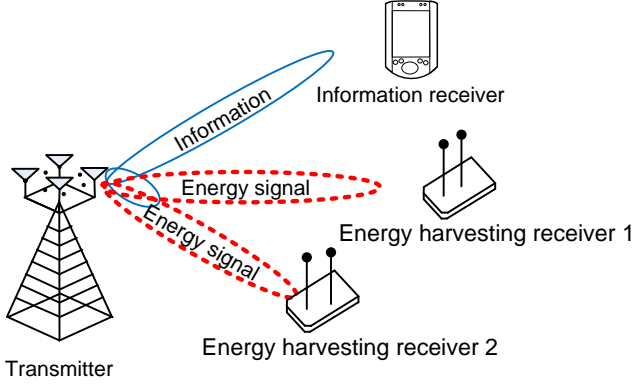


Fig. 1. A downlink communication system with an information receiver (IR) and $J = 2$ energy harvesting receivers (ERs).

networks.

A. Notation

\mathbf{A}^H , $\text{Tr}(\mathbf{A})$, and $\text{Rank}(\mathbf{A})$ represent the Hermitian transpose, trace, and rank of matrix \mathbf{A} ; $\mathbf{A} \succeq \mathbf{0}$ indicates that \mathbf{A} is a positive semidefinite matrix; matrix \mathbf{I}_N denotes an $N \times N$ identity matrix. $\text{vec}(\mathbf{A})$ denotes the vectorization of matrix \mathbf{A} by stacking its columns from left to right to form a column vector. $\mathbf{A} \otimes \mathbf{B}$ denotes the Kronecker product of matrices \mathbf{A} and \mathbf{B} . $[\mathbf{B}]_{a:b, c:d}$ returns the a -th to the b -th rows and the c -th to the d -th columns block submatrix of \mathbf{B} . $\mathbb{C}^{N \times M}$ denotes the space of $N \times M$ matrices with complex entries. \mathbb{H}^N represents the set of all N -by- N complex Hermitian matrices. The distribution of a circularly symmetric complex Gaussian (CSCG) vector with mean vector \mathbf{x} and covariance matrix Σ is denoted by $\mathcal{CN}(\mathbf{x}, \Sigma)$, and \sim means “distributed as”. $\mathcal{E}\{\cdot\}$ denotes statistical expectation. $\|\cdot\|$ and $\|\cdot\|_F$ denote the Euclidean norm and the Frobenius norm of a vector/matrix, respectively. $\text{Re}(\cdot)$ extracts the real part of a complex-valued input.

B. Channel Model

We focus on a downlink SWIPT system. The system consists of a transmitter, a single-antenna information receiver (IR), and multiple energy harvesting receivers (ERs). The transmitter is equipped with N_T antennas and each ER is equipped with N_R receiving antennas. We assume that the ERs are roaming wireless terminals from other communication systems searching for additional power supply in the RF. The transmission is divided into time slots. In each time slot, the transmitter sends a precoded information signal and an energy signal simultaneously to facilitate information transmission to the IR and power transfer to the ERs, cf. Figure 1. The transmit signal is given by

$$\mathbf{x} = \mathbf{w}_I s + \mathbf{w}_E, \quad (1)$$

where $s \in \mathbb{C}$ is the information-bearing symbol with $\mathcal{E}\{|s|^2\} = 1$ and $\mathbf{w}_I \in \mathbb{C}^{N_T \times 1}$ is the corresponding information beamforming vector. $\mathbf{w}_E \in \mathbb{C}^{N_T \times 1}$ is the energy signal facilitating energy transfer to the ERs. The energy signal \mathbf{w}_E is a deterministic pseudo-random sequence with zero mean and covariance matrix \mathbf{W}_E . Since \mathbf{w}_E is generated at the transmitter by a pseudo-random sequence generator with a predefined seed, the energy signal is known to the IR. Thus,

the interference caused by the energy signal can be completely cancelled at the IR.

We assume a narrow-band slow fading channel between the transmitter and receivers. Then, the received signals at the IR and ER j are expressed as

$$y^{\text{IR}} = \mathbf{h}^H (\mathbf{w}_I s + \mathbf{w}_E) + n_I, \quad (2)$$

$$\mathbf{y}_j^{\text{ER}} = \mathbf{G}_j^H (\mathbf{w}_I s + \mathbf{w}_E) + \mathbf{n}_j^E, \quad (3)$$

where $\mathbf{h} \in \mathbb{C}^{N_T \times 1}$ is the channel vector between the transmitter and the IR, and $\mathbf{G}_j \in \mathbb{C}^{N_T \times N_R}$ is the channel matrix between the transmitter and ER j . Variables \mathbf{h} and \mathbf{G}_j capture the joint effect of multipath fading and path loss. $n_I \in \mathbb{C}$ and $\mathbf{n}_j^E \in \mathbb{C}^{N_R \times 1}$ are additive white Gaussian noises (AWGNs) at the IR and ER j , respectively, and are distributed as $\mathcal{CN}(0, \sigma_I^2)$ and $\mathcal{CN}(\mathbf{0}, \sigma_E^2 \mathbf{I}_{N_R})$.

III. RESOURCE ALLOCATION ALGORITHM DESIGN

In this section, we present the adopted performance metrics and the problem formulation.

A. Achievable Rate, Harvested Energy, and Energy Efficiency

The achievable rate (bit-per-second) at the IR is given by

$$R = B \log_2 \left(1 + \frac{\mathbf{w}_I^H \mathbf{H} \mathbf{w}_I}{\sigma_I^2} \right), \quad (4)$$

where B is the system bandwidth and $\mathbf{H} = \mathbf{h} \mathbf{h}^H$. We note that the interference caused by the energy signal, i.e., $\text{Tr}(\mathbf{w}_E^H \mathbf{H} \mathbf{w}_E)$, is removed from the IR via successive interference cancellation before the IR decodes the desired information since the energy signal \mathbf{w}_E is known to the receiver. On the other hand, both the information signal and the energy signal can act as RF energy sources for the ER due to the broadcast nature of wireless channels. As a result, the total harvested energy¹ at ER j is given by

$$P_j^{\text{harv}} = \eta_j \text{Tr} \left(\mathbf{G}_j^H (\mathbf{w}_I \mathbf{w}_I^H + \mathbf{W}_E) \mathbf{G}_j \right), \quad (5)$$

and η_j is the energy conversion efficiency of ER j which is a constant with $0 \leq \eta_j \leq 1$ and models the energy loss of the process of converting the received RF energy to electrical energy for storage. We ignore the thermal noise at the receiving antenna for energy harvesting as it is relatively small compared to the received signal power.

Energy efficiency is a fundamental system performance metric in modern communication networks. To design a resource allocation algorithm for energy-efficient communication, the total power consumption has to be included in the optimization objective function. Thus, we model the power dissipation (Joule-per-second) in the system as

$$P_{\text{tot}} = \frac{\|\mathbf{w}_I\|^2 + \text{Tr}(\mathbf{W}_E)}{\xi} + P_B, \quad (6)$$

$$\text{where } P_B = N_T P_{\text{ant}} + P_c. \quad (7)$$

$0 < \xi \leq 1$ is the constant power amplifier efficiency. The first term in (6) is the total power consumption in the power

¹We note that a normalized energy unit, i.e., Joule-per-second, is adopted. Therefore, the terms “power” and “energy” are used interchangeably in this paper.

amplifier. $N_T P_{\text{ant}}$ in (7) accounts for the dynamic circuit power consumption which is proportional to the number of transmit antennas. P_{ant} denotes the power dissipation at each transmit antenna, including the dissipation in the transmit filter, mixer, frequency synthesizer, digital-to-analog converter (DAC), etc. P_c denotes the fixed circuit power consumption for baseband signal processing.

Therefore, the achievable rate energy efficiency (AR-EE) and the energy transfer energy efficiency (ET-EE) of the considered system are defined as

$$\Phi_{\text{IR}} = \frac{B \log_2(1 + \frac{\mathbf{w}_I^H \mathbf{H} \mathbf{w}_I}{\sigma_I^2})}{(\|\mathbf{w}_I\|^2 + \text{Tr}(\mathbf{W}_E))/\xi + N_T P_{\text{ant}} + P_c} \quad \text{and} \quad (8)$$

$$\Phi_{\text{EH}} = \frac{\sum_j P_j^{\text{harv}}}{(\|\mathbf{w}_I\|^2 + \text{Tr}(\mathbf{W}_E))/\xi + N_T P_{\text{ant}} + P_c}, \quad (9)$$

respectively, where P_j^{harv} is given in (5).

B. Channel State Information (CSI)

In this paper, we focus on a Time Division Duplex (TDD) communication system with slowly time-varying channels. At the beginning of each time slot, handshaking is performed between the transmitter and the IR. As a result, the downlink CSI of the IR can be obtained by measuring the uplink training sequences embedded in the handshaking signals. Thus, we assume that the transmitter-to-IR fading gain, \mathbf{h} , can be estimated perfectly at the transmitter. On the other hand, the ERs may not directly interact with the transmitter. Besides, the ERs may be silent for long periods of time. As a result, the CSI of the ERs can be obtained only occasionally at the transmitter when the ERs communicate with the transmitter. Hence, the CSI for the ERs may be outdated when the transmitter performs resource allocation. We adopt a deterministic model [14], [15] to characterize the impact of the CSI imperfection for resource allocation design. The CSI of the link between the transmitter and ER j is modeled as

$$\mathbf{G}_j = \hat{\mathbf{G}}_j + \Delta \mathbf{G}_j, \quad \forall j \in \{1, \dots, J\}, \quad \text{and} \quad (10)$$

$$\Psi_j \triangleq \left\{ \Delta \mathbf{G}_j \in \mathbb{C}^{N_T \times N_R} : \|\Delta \mathbf{G}_j\|_F^2 \leq \varepsilon_j^2 \right\}, \quad \forall j, \quad (11)$$

where $\hat{\mathbf{G}}_j \in \mathbb{C}^{N_T \times N_R}$ is the matrix CSI estimate of the channel of ER j that is available at the transmitter. $\Delta \mathbf{G}_j$ represents the unknown channel uncertainty and the continuous set Ψ_j in (11) defines a continuous space spanned by all possible channel uncertainties. Constant ε_j represents the maximum value of the norm of the CSI estimation error matrix $\Delta \mathbf{G}_j$ for ER j .

IV. PROBLEM FORMULATION AND SOLUTION

A. Problem Formulation

In SWIPT systems, AR-EE maximization and ET-EE maximization are both desirable system design objectives. In this section, we first propose two problem formulations for single-objective system design for SWIPT. Each single-objective problem describes one important aspect of the system design. Then, we consider both system design objectives jointly via the multi-objective problem formulation.

The first system design objective is the maximization of AR-EE without the consideration of energy harvesting. The corresponding optimization problem is formulated² as

Problem 1: AR-EE Maximization:

$$\begin{aligned} & \underset{\mathbf{W}_E \in \mathbb{H}^{N_T}, \mathbf{w}_I}{\text{maximize}} && \Phi_{\text{IR}} \\ & \text{subject to} && \text{C1: } \|\mathbf{w}_I\|^2 + \text{Tr}(\mathbf{W}_E) \leq P_{\text{max}}, \\ & && \text{C2: } \mathbf{W}_E \succeq \mathbf{0} \end{aligned} \quad (12)$$

P_{max} in constraint C1 denotes the maximum transmit power budget. In addition, covariance matrix \mathbf{W}_E is a positive semidefinite Hermitian matrix as indicated by constraint C2.

The second system design objective is the maximization of the ET-EE. The corresponding problem formulation is given as

Problem 2: ET-EE Maximization:

$$\begin{aligned} & \underset{\mathbf{W}_E \in \mathbb{H}^{N_T}, \mathbf{w}_I}{\text{maximize}} && \min_{\Delta \mathbf{G}_j \in \Psi_j} \Phi_{\text{EH}} \\ & \text{subject to} && \text{C1, C2.} \end{aligned} \quad (13)$$

For the sake of notational simplicity, we denote the objective functions in the above problems as F_n , $n = 1, 2$. In practice, these two system design objectives are both desirable from the system operator perspective. However, it is expected that there is a non-trivial trade-off between these objectives. In order to meet these conflicting system design objectives systematically and simultaneously, we adopt the weighted Tchebycheff method for the multi-objective optimization [16] which can provide the complete Pareto optimal set by varying predefined preference parameters. To this end, we incorporate the two individual system design objectives into a multi-objective optimization problem (MOOP), which is formulated as

Problem 3: Multi-Objective Optimization Problem:

$$\begin{aligned} & \underset{\mathbf{W}_E \in \mathbb{H}^{N_T}, \mathbf{w}_I}{\text{minimize}} && \max_{i=1,2} \left\{ \omega_i (F_i^* - F_i) \right\} \\ & \text{subject to} && \text{C1, C2,} \end{aligned} \quad (14)$$

where F_i^* is the optimal objective value with respect to Problem i . ω_i is a weight imposed on objective function i subject to $0 \leq \omega_i \leq 1$ and $\sum_i \omega_i = 1$, which indicates the preference of the system designer for the i -th objective function over the others. In the extreme case, when $\omega_i = 1$ and $\omega_n = 0, \forall n \neq i$, Problem 3 is equivalent to single-objective optimization problem i .

²We note that the considered problem formulation can be easily extended to the case with a minimum data rate requirement. Yet, a stringent data rate requirement does not facilitate the study the trade-off between different system objectives due to the resulting smaller feasible solution set.

V. OPTIMIZATION SOLUTIONS

It can be observed that the objective functions of Problems 1–3 are non-convex functions. In general, there is no well-known systematical approach for solving non-convex optimization problems. In order to obtain a tractable solution, we first transform the non-convex objective functions using the Charnes-Cooper transformation. Then, we use semidefinite programming relaxation (SDR) to obtain the resource allocation solution for the reformulated problem.

We first reformulate the aforementioned three optimization problems by defining a set of new optimization variables:

$$\begin{aligned}\mathbf{W}_I &= \mathbf{w}_I \mathbf{w}_I^H, \theta = \frac{1}{P_{\text{tot}}}, \\ \overline{\mathbf{W}}_I &= \theta \mathbf{W}_I, \text{ and } \overline{\mathbf{W}}_E = \theta \mathbf{W}_E.\end{aligned}\quad (15)$$

Then, the original problems can be rewritten with respect to the new optimization variables $\{\overline{\mathbf{W}}_I, \overline{\mathbf{W}}_E, \theta\}$. Problem 1 becomes

Problem 4: Transformed AR-EE Maximization Problem:

$$\begin{aligned}& \underset{\overline{\mathbf{W}}_I, \overline{\mathbf{W}}_E \in \mathbb{H}^{N_T}, \theta}{\text{maximize}} && \theta \log_2 \left(1 + \frac{\text{Tr}(\mathbf{H} \overline{\mathbf{W}}_I)}{\theta \sigma_I^2} \right) \\ & \text{subject to} && \overline{\text{C1}} : \text{Tr}(\overline{\mathbf{W}}_I + \overline{\mathbf{W}}_E) \leq \theta P_{\text{max}}, \\ & && \overline{\text{C2}} : \overline{\mathbf{W}}_I \succeq \mathbf{0}, \overline{\mathbf{W}}_E \succeq \mathbf{0}, \\ & && \overline{\text{C3}} : \text{Rank}(\overline{\mathbf{W}}_I) \leq 1, \\ & && \overline{\text{C4}} : \frac{\text{Tr}(\overline{\mathbf{W}}_I + \overline{\mathbf{W}}_E)}{\xi} + \theta P_B \leq 1, \\ & && \overline{\text{C5}} : \theta \geq 0,\end{aligned}\quad (16)$$

where $\overline{\mathbf{W}}_I \succeq \mathbf{0}, \overline{\mathbf{W}}_I \in \mathbb{H}^{N_T}$, and $\overline{\text{C3}}$ are imposed to guarantee that $\overline{\mathbf{W}}_I = \theta \mathbf{w}_I \mathbf{w}_I^H$. Constant B is dropped from the objective function in Problem 4 since it is independent of the optimization variables. Similarly, Problem 2 becomes

Problem 5: Transformed ET-EE Maximization Problem:

$$\begin{aligned}& \underset{\overline{\mathbf{W}}_I, \overline{\mathbf{W}}_E \in \mathbb{H}^{N_T}, \theta, \gamma_j}{\text{maximize}} && \sum_{j=1}^J \gamma_j \\ & \text{subject to} && \overline{\text{C1}} - \overline{\text{C5}}, \\ & && \overline{\text{C6}} : \gamma_j \leq \min_{\Delta \mathbf{G}_j \in \Psi_j} P_j^{\text{harv}}, \forall j,\end{aligned}\quad (17)$$

where γ_j are auxiliary optimization variables.

Finally, Problem 3 can be written as

Problem 6: Transformed MOOP:

$$\begin{aligned}& \underset{\overline{\mathbf{W}}_I, \overline{\mathbf{W}}_E \in \mathbb{H}^{N_T}, \theta, \tau}{\text{minimize}} && \tau \\ & \text{subject to} && \overline{\text{C1}} - \overline{\text{C6}}, \\ & && \overline{\text{C7}} : \omega_i(F_i^* - F_i) \leq \tau, i \in \{4, 5\},\end{aligned}\quad (18)$$

where τ is an auxiliary optimization variable.

Proposition 1: The Problems 4–6 are equivalent transformations of the original Problems 1–3, respectively.

Proof: The transformation is based on Charnes-Cooper transformation. Due to the space limitation, we refer to [16] for proof for a similar problem. ■

We note that Problem 6 is a generalization of Problems 4 and 5. If Problem 6 can be solved optimally by an algorithm, then the algorithm can also be used to solve Problems 4 and 5. Thus, we focus on the method for solving³ Problem 6. It is evident that Problem 6 is non-convex due to the rank-one beamforming matrix constraint $\overline{\text{C3}} : \text{Rank}(\overline{\mathbf{W}}_I) \leq 1$. Besides, constraint $\overline{\text{C6}}$ involves infinitely many constraints due to the continuous uncertainty set Ψ_j . Next, we introduce a Lemma which allows us to transform constraint $\overline{\text{C6}}$ into a finite number of linear matrix inequalities (LMIs) constraints.

Lemma 1 (S-Procedure [17]): Let a function $f_m(\mathbf{x}), m \in \{1, 2\}, \mathbf{x} \in \mathbb{C}^{N \times 1}$, be defined as

$$f_m(\mathbf{x}) = \mathbf{x}^H \mathbf{A}_m \mathbf{x} + 2\text{Re}\{\mathbf{b}_m^H \mathbf{x}\} + c_m, \quad (19)$$

where $\mathbf{A}_m \in \mathbb{H}^N$, $\mathbf{b}_m \in \mathbb{C}^{N \times 1}$, and $c_m \in \mathbb{R}$. Then, the implication $f_1(\mathbf{x}) \leq 0 \Rightarrow f_2(\mathbf{x}) \leq 0$ holds if and only if there exists an $\omega \geq 0$ such that

$$\omega \begin{bmatrix} \mathbf{A}_1 & \mathbf{b}_1 \\ \mathbf{b}_1^H & c_1 \end{bmatrix} - \begin{bmatrix} \mathbf{A}_2 & \mathbf{b}_2 \\ \mathbf{b}_2^H & c_2 \end{bmatrix} \succeq \mathbf{0}, \quad (20)$$

provided that there exists a point $\hat{\mathbf{x}}$ such that $f_k(\hat{\mathbf{x}}) < 0$.

Now, we apply Lemma 1 to constraint $\overline{\text{C6}}$. In particular, we define $\hat{\mathbf{g}}_j = \text{vec}(\hat{\mathbf{G}}_j)$, $\Delta \mathbf{g}_j = \text{vec}(\Delta \mathbf{G}_j)$, $\widetilde{\mathbf{W}}_I = \mathbf{I}_{N_R} \otimes \overline{\mathbf{W}}_I$, and $\widetilde{\mathbf{W}}_E = \mathbf{I}_{N_R} \otimes \overline{\mathbf{W}}_E$. By exploiting the fact that $\|\Delta \mathbf{G}_j\|_F^2 \leq \varepsilon_j^2 \Leftrightarrow \Delta \mathbf{g}_j^H \Delta \mathbf{g}_j \leq \varepsilon_j^2$, then we have

$$\begin{aligned}& \|\Delta \mathbf{G}_j\|_F^2 \leq \varepsilon_j^2 \\ \Rightarrow & \overline{\text{C6}} : 0 \geq \gamma_j + \min_{\Delta \mathbf{g}_j \in \Psi_j} -\left\{ \Delta \mathbf{g}_j^H (\widetilde{\mathbf{W}}_I + \widetilde{\mathbf{W}}_E) \Delta \mathbf{g}_j \right. \\ & \left. + 2\text{Re}\{\hat{\mathbf{g}}_j^H (\widetilde{\mathbf{W}}_I + \widetilde{\mathbf{W}}_E) \Delta \mathbf{g}_j\} + \hat{\mathbf{g}}_j^H (\widetilde{\mathbf{W}}_I + \widetilde{\mathbf{W}}_E) \hat{\mathbf{g}}_j \right\}, \forall j,\end{aligned}\quad (21)$$

if and only if there exists a $\rho_j \geq 0$ such that the following LMIs constraint holds:

$$\begin{aligned}\overline{\text{C6}} : \mathbf{S}_{\overline{\text{C6}}_j} &= \begin{bmatrix} \rho_j \mathbf{I}_{N_T} + \widetilde{\mathbf{W}}_E & \widetilde{\mathbf{W}}_E \hat{\mathbf{g}}_j \\ \hat{\mathbf{g}}_j^H \widetilde{\mathbf{W}}_E & -\rho_j \varepsilon_j^2 - \frac{\gamma_j}{\eta_j} + \hat{\mathbf{g}}_j^H \widetilde{\mathbf{W}}_E \hat{\mathbf{g}}_j \end{bmatrix} \\ &+ \mathbf{U}_{\mathbf{g}_j}^H \widetilde{\mathbf{W}}_I \mathbf{U}_{\mathbf{g}_j} \succeq \mathbf{0}, \forall j,\end{aligned}\quad (22)$$

where $\mathbf{U}_{\mathbf{g}_j} = [\mathbf{I}_{N_R N_T}, \hat{\mathbf{g}}_j]$. The new constraint $\overline{\text{C6}}$ is not only an affine function with respect to the optimization variables, but also involves only a finite number of constraints. Then, we apply the SDP relaxation by removing constraint $\overline{\text{C3}}$ from Problem 6. As a result, the SDP relaxed problem is given by

³In studying the solution structure of Problem 6, we assume that the optimal objective values of Problems 4, 5 are given constants, i.e., $F_p^*, \forall p \in \{4, 5\}$, are known. Once the structure of the optimal resource allocation scheme of Problem 6 is obtained, it can be exploited to obtain the optimal solution of Problems 4, 5.

TABLE I
SIMULATION PARAMETERS

Carrier center frequency	915 MHz
Bandwidth	200 kHz
Single antenna power consumption	$P_{\text{ant}} = 1$ W
Static circuit power consumption	$P_c = 150$ W [19]
Power amplifier efficiency	$\xi = 0.2$
Transmit antenna gain	18 dBi
Noise power	$\sigma^2 = -95$ dBm
Transmitter-to-ERs fading distribution	Rician with Rician factor 6 dB
Transmitter-to-IR fading distribution	Rayleigh
Energy conversion efficiency	$\eta_j = 0.5$

Problem 7: SDP Relaxed Transformed MOOP:

$$\begin{aligned}
 & \underset{\mathbf{\bar{W}}_I, \mathbf{\bar{W}}_E \in \mathbb{H}^{N_T}, \theta, \tau, \gamma_j, \rho_j}{\text{minimize}} && \tau \\
 & \text{subject to} && \overline{C1}, \overline{C2}, \overline{C4}, \overline{C5}, \overline{C7}, \\
 & && \overline{C6} : \mathbf{S}_{\overline{C6}_j} \succeq \mathbf{0}, \overline{C8} : \rho_j \geq 0, \forall j,
 \end{aligned} \tag{23}$$

which is a convex SDP problem and can be solved by numerical convex program solvers such as CVX [18]. In particular, if the obtained solution $\mathbf{\bar{W}}_I^*$ of the SDP relaxed problem satisfies constraint $\overline{C3}$, i.e., $\text{Rank}(\mathbf{\bar{W}}_I^*) \leq 1$, then it is the optimal solution. Now, we study the tightness of the SDP relaxation by the following theorem.

Theorem 1: Assuming that the channels, i.e., \mathbf{h} and \mathbf{G}_j , are statistically independent and Problem 7 is feasible, the optimal beamforming matrix of Problem 7 is a rank-one matrix with probability one, i.e., $\text{Rank}(\mathbf{\bar{W}}_I^*) \leq 1$. Besides, for $\omega_1 > 0$, the optimal energy signal is $\mathbf{\bar{W}}_E^* = \mathbf{0}$.

Proof: Please refer to the Appendix. ■

Therefore, the adopted SDP relaxation is tight. Besides, whenever AR-EE is considered, i.e., $\omega_1 > 0$, no dedicated energy beam is needed. In fact, the optimal information beam, $\mathbf{\bar{W}}_I$, serves as a dual purpose carrier for maximization of the energy efficiency of information transmission and WPT simultaneously. Furthermore, Problems 1-2 can be solved by SDP relaxation as solving Problem 7.

VI. RESULTS

In this section, we present simulation results to demonstrate the system performance of multi-objective SWIPT system design. The simulation parameters are summarized in Table I. The IR and J ERs are located 100 meters and 10 meters from the transmitter. In particular, the ERs are near the transmitter with line-of-sight communication channels to facilitate energy harvesting. Each ER is equipped with $N_R = 2$ antennas for facilitating EH. We assume that the noise powers at each antenna of the IR and the ERs are identical, i.e., $\sigma_I^2 = \sigma_E^2 = \sigma^2$. In the sequel, we define the normalized maximum channel estimation error of ER j as $\delta_j^2 = \frac{\epsilon_j^2}{\|\mathbf{G}_j\|_F^2}$ with $\delta_a^2 = \delta_b^2 = 0.05, \forall a, b \in \{1, \dots, J\}$. All simulation results are obtained by averaging the system performance over different multipath channel realizations.

Figure 2 depicts the trade-off region for the average ET-EE and the average AR-EE achieved by the proposed optimal

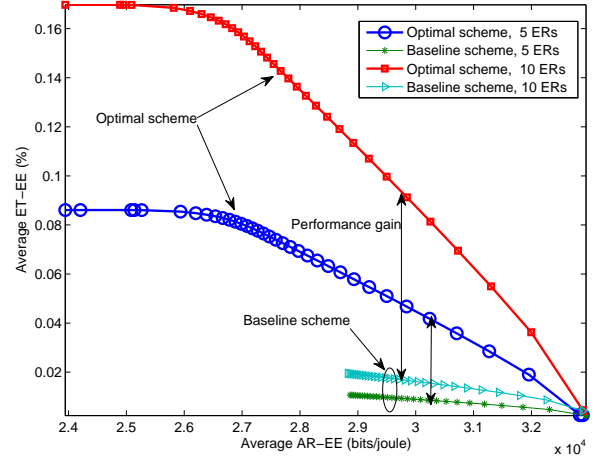


Fig. 2. System performance trade-off region between the average ET-EE and the average AR-EE for $P_{\text{max}} = 40$ dBm. The double-sided arrows indicate the performance gain achieved by the proposed optimal scheme over the baseline scheme.

scheme for different numbers of ERs. The maximum transmit power is set to $P_{\text{max}} = 40$ dBm. The trade-off region in Figure 2 is obtained by solving Problem 7 via varying the values of $0 \leq \lambda_p \leq 1, \forall p \in \{1, 2\}$, uniformly for a step size of 0.01 such that $\sum_p \lambda_p = 1$. It can be observed that the ET-EE is a monotonically decreasing function with respect to the AR-EE. The result indicates that AR-EE maximization and ET-EE maximization are conflicting system design objectives in general. In other words, a resource allocation algorithm maximizing the AR-EE cannot maximize the ET-EE simultaneously in the considered system. Besides, the trade-off region is enlarged for an increasing number of ERs. This is due to the fact that a larger portion of the radiated power can be harvested when there are more ERs in the system since more receivers participate in the energy harvesting process.

For comparison, we also plot the trade-off region of a baseline power allocation scheme in Figure 2. For the baseline scheme, the covariance matrix of the energy signal $\mathbf{\bar{W}}_E$ is set to zero. Then, maximum ratio transmission (MRT) with respect to the IR is adopted for the information beamforming matrix $\mathbf{\bar{W}}_I$. In other words, the beamforming direction of matrix $\mathbf{\bar{W}}_I$ is fixed. Then, we optimize the power of $\mathbf{\bar{W}}_I$ subject to the constraints in Problem 7. It can be observed that the baseline scheme achieves a significantly smaller trade-off region compared to the proposed optimal scheme. As a matter of fact, the degrees of freedom of the beamforming matrix $\mathbf{\bar{W}}_I$ are jointly optimized in our proposed optimal scheme via utilizing the CSI of all receivers. On the contrary, the information beamformer in the baseline scheme is restricted to the range space of the IR. Although the baseline scheme is optimal when AR-EE is the only system design objective, the information beamformer cannot be steered towards the direction of the ERs. Thus, compared to the proposed optimal scheme, the baseline scheme is less efficient when ET-EE is considered.

Figures 3 and 4 illustrate the average AR-EE and the average ET-EE versus the total transmit power budget P_{max} ,

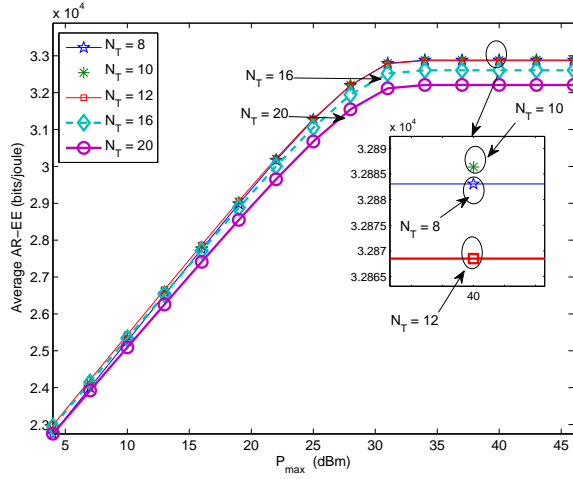


Fig. 3. Average AR-EE (bits/joule) versus maximum transmit power budget P_{\max} (dBm).

respectively, for $J = 10$ ERs. The results in Figures 3 and 4 are obtained by solving Problem 7 with $\{\omega_1 = 1, \omega_2 = 0\}$ and $\{\omega_1 = 0, \omega_2 = 1\}$, respectively. It can be observed from Figure 3 that the AR-EE of the proposed optimal scheme increases with respect to P_{\max} monotonically and reaches an upper limit where the EE gain due to a higher value of P_{\max} vanishes. This result indicates that once the maximum AR-EE is achieved by transmitting a sufficiently large power, any additional increase in the transmitted power will incur a loss in EE which is prevented by the optimal algorithm. On the other hand, it can be seen from Figure 4 that the average ET-EE increases slowly in the low transmit power regime but increases rapidly in the high transmit power regime. This is because for a small transmit power, the ET-EE is dominated by the fixed circuit power consumption, P_B , leading to a slow increasing rate of ET-EE with respect to the transmit power. As the transmit power budget increases, the transmit power consumption in the RF becomes significant and the ET-EE becomes more sensitive to increases in transmit power budget, cf. (9). On the other hand, the number of transmit antennas N_T affects the AR-EE and the ET-EE differently. In fact, the maximum AR-EE does not necessarily increase with the number of transmit antennas when the per-antenna power consumption is considered, cf. Figure 3. This is because the AR scales logarithmically with respect to the number of transmit antennas. However, the AR gain due to extra transmit antennas is not sufficient to compensate the total increased energy cost since the circuit power consumption increases linearly with respect to N_T . Thus, adopting exceedingly large numbers of transmit antennas may not be a viable solution for information transmission. In contrast, the maximum ET-EE increases with N_T as shown in Figure 4. This is due to the fact that the ET-EE function in (9) is a quasi-linear function with respect to both $\bar{\mathbf{W}}_I$ and $\bar{\mathbf{W}}_E$. Thus, a large number of transmit antennas is beneficial if ET-EE is the only system design objective.

VII. CONCLUSIONS

In this paper, we studied the resource allocation algorithm design for energy-efficient SWIPT networks. The algorithm

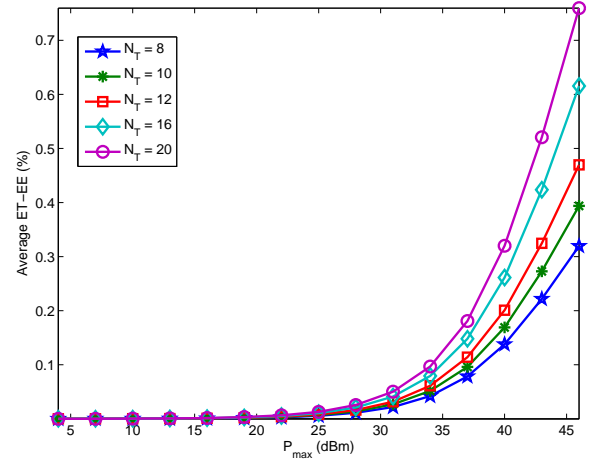


Fig. 4. Average ET-EE versus maximum transmit power budget P_{\max} (dBm).

design was formulated as a non-convex MOOP employing the weighted Tchebycheff method. The proposed problem aimed at the joint maximization of the energy efficiency of information transmission and WPT simultaneously. Besides, the imperfectness of the CSI of the ERs was also taken into account for designing a robust resource allocation algorithm. The proposed MOOP was solved optimally by SDP relaxation. Simulation results not only reveal the trade-off between the studied conflicting systems design objectives, but also shed some light on the use of multiple transmit antennas for improving system energy efficiency.

APPENDIX-PROOF OF THEOREM 1

Since Problem 7 satisfies Slater's constraint qualification and is jointly convex with respect to the optimization variables, strong duality holds. Thus, solving the dual problem is equivalent to solving the primal problem. Therefore, Theorem 1 can be proved by analyzing the dual problem of Problem 7. To this end, we define the Lagrangian function \mathcal{L}

$$\begin{aligned} \mathcal{L} = & \tau + \alpha (\text{Tr}(\bar{\mathbf{W}}_I + \bar{\mathbf{W}}_E) - \theta P_{\max}) - \delta \theta \\ & + \beta \left(\frac{\text{Tr}(\bar{\mathbf{W}}_I + \bar{\mathbf{W}}_E)}{\xi} + \theta P_B - 1 \right) \\ & + v_1 \left[\omega_1 (F_1^* - \theta \log_2(1 + \frac{\text{Tr}(\mathbf{H}\bar{\mathbf{W}}_I)}{\theta \sigma_I^2})) - \tau \right] \\ & + v_2 \left[\omega_2 (F_2^* - \sum_{j=1}^J \gamma_j) - \tau \right] - \text{Tr}(\mathbf{X}\bar{\mathbf{W}}_I) - \text{Tr}(\mathbf{Y}\bar{\mathbf{W}}_E) \\ & - \sum_{j=1}^J \text{Tr}(\mathbf{D}_{\bar{\mathbf{C}}_{6j}} \mathbf{S}_{\bar{\mathbf{C}}_{6j}}) - \sum_{j=1}^J \mu_j \rho_j, \end{aligned} \quad (24)$$

where $\alpha, \beta, \delta, \mu_j \geq 0$ are dual variables associated with constraints C1, C4, C5, and C8, respectively. Dual variable matrices \mathbf{X} , \mathbf{Y} , and $\mathbf{D}_{\bar{\mathbf{C}}_{6j}}$ are connected to the LMI constraints in C2 and C6, respectively. v_1, v_2 are the dual variables for constraint C7.

Then, the dual problem of Problem 7 is given by

$$\begin{aligned} & \underset{\alpha, \beta, \delta, \mu_j \geq 0, \mathbf{Y}, \mathbf{X}, \mathbf{D}_{\bar{\mathbf{C}}_{6j}} \geq 0}{\text{maximize}} & \underset{\substack{\bar{\mathbf{W}}_I, \bar{\mathbf{W}}_E \in \mathbb{H}^{N_T}, \\ \theta, \tau, \gamma_j, \rho_j}}{\text{minimize}} & \mathcal{L}. \end{aligned} \quad (25)$$

Now, we focus on those Karush-Kuhn-Tucker (KKT) conditions which are useful for the proof:

$$\mathbf{Y}, \mathbf{X}, \mathbf{D}_{\overline{\mathbf{C}}_j} \succeq \mathbf{0}, \alpha, \beta, \delta, \mu_j \geq 0, \forall j, \quad (26)$$

$$\mathbf{X} = \mathbf{Y} - \frac{v_1 \omega_1 \theta}{\theta \sigma_1^2 + \text{Tr}(\mathbf{H}\overline{\mathbf{W}}_1)} \mathbf{H}, \quad (27)$$

$$\mathbf{Y} = (\alpha + \frac{\beta}{\xi}) \mathbf{I}_{N_T} - \sum_{j=1}^J \sum_{l=1}^{N_R} [\mathbf{U}_{\mathbf{g}_j} \mathbf{D}_{\overline{\mathbf{C}}_j} \mathbf{U}_{\mathbf{g}_j}^H]_{a:b,c:d}, \quad (28)$$

$$\mathbf{X}\overline{\mathbf{W}}_1 = \mathbf{0}, \quad (29)$$

$$\mathbf{Y}\overline{\mathbf{W}}_E = \mathbf{0}. \quad (30)$$

where $a = (l-1)N_T + 1, b = lN_T, c = (l-1)N_T + 1$, and $d = lN_T$. Next, we investigate the structure of $\overline{\mathbf{W}}_1$ in the following two cases.

Case 1: For $\omega_1 = 0$ and $\omega_2 = 1$, AR-EE maximization is not considered and ET-EE maximization is the only system design objective. Besides, since $\omega_1 = 0$, we have $\mathbf{X} = \mathbf{Y}$. In other words, $\overline{\mathbf{W}}_1$ has the same functionality as $\overline{\mathbf{W}}_E$ for improving the ET-EE. Thus, without loss of generality and optimality, we can set $\overline{\mathbf{W}}_1 = \mathbf{0}$ and $\text{Rank}(\overline{\mathbf{W}}_1) \leq 1$ holds for the optimal solution.

Case 2: For $\omega_1 > 0$, AR-EE maximization is considered in the resource allocation algorithm design. Thus, constraint $\overline{\mathbf{C}}_6$ for $j = 1$ is active, i.e., $v_1 > 0$. Besides, from the complementary slackness condition in (29), the columns of $\overline{\mathbf{W}}_1$ for the optimal solution lie in the null space of \mathbf{X} for $\overline{\mathbf{W}}_1 \neq \mathbf{0}$. Therefore, if $\text{Rank}(\mathbf{X}) = N_T - 1$, then the optimal beamforming matrix must be a rank-one matrix. To reveal the structure of \mathbf{X} , we show by contradiction that \mathbf{Y} is a positive definite matrix with probability one. For a given set of optimal dual variables, $\{\mathbf{Y}, \mathbf{X}, \mathbf{D}_{\overline{\mathbf{C}}_j}, \alpha, \beta, \delta, \mu_j\}$, and optimal primal variables $\{\tau, \gamma_j, \theta, \overline{\mathbf{W}}_E, \rho_j\}$, (25) can be written as

$$\underset{\overline{\mathbf{W}}_1 \in \mathbb{H}^{N_T}}{\text{minimize}} \mathcal{L}. \quad (31)$$

Suppose \mathbf{Y} is not positive definite, then we can construct $\overline{\mathbf{W}}_1 = r\mathbf{v}\mathbf{v}^H$ as one of the optimal solutions of (31), where $r > 0$ is a scaling parameter and \mathbf{v} is the eigenvector corresponding to one of the non-positive eigenvalues of \mathbf{Y} . We substitute $\overline{\mathbf{W}}_1 = r\mathbf{v}\mathbf{v}^H$ into (31) which leads to $\mathcal{L} = \text{Tr}(r\mathbf{Y}\mathbf{v}\mathbf{v}^H) - r\text{Tr}\left(\mathbf{v}\mathbf{v}^H\left(\mathbf{X} + \frac{v_1\omega_1\theta\mathbf{H}}{\theta\sigma_1^2 + \text{Tr}(\mathbf{H}\overline{\mathbf{W}}_1)}\right)\right) + \Omega$ where Ω is the collection of variables that are independent of $\overline{\mathbf{W}}_1$. Since the channels of \mathbf{G}_j and \mathbf{h} are assumed to be statistically independent, it follows that by setting $r \rightarrow \infty$, the dual optimal value becomes unbounded from below. Besides, the optimal value of the primal problem is non-negative. Thus, this leads to a contradiction since strong duality does not hold. Therefore, \mathbf{Y} is a positive definite matrix with probability one, i.e., $\text{Rank}(\mathbf{Y}) = N_T$.

By exploiting (27) and a basic inequality for the rank of matrices, we have

$$\text{Rank}(\mathbf{X}) + \text{Rank}\left(\frac{v_1\omega_1\theta\mathbf{H}}{\theta\sigma_1^2 + \text{Tr}(\mathbf{H}\overline{\mathbf{W}}_1)}\right) \quad (32)$$

$$\geq \text{Rank}(\mathbf{Y}) = N_T \quad (33)$$

$$\Rightarrow \text{Rank}(\mathbf{X}) \geq N_T - \text{Rank}\left(\frac{v_1\omega_1\theta\mathbf{H}}{\theta\sigma_1^2 + \text{Tr}(\mathbf{H}\overline{\mathbf{W}}_1)}\right). \quad (34)$$

Furthermore, $\overline{\mathbf{W}}_1 \neq \mathbf{0}$ is required to maximize the energy efficiency of data communication. Hence, $\text{Rank}(\mathbf{X}) = N_T - 1$ and $\text{Rank}(\overline{\mathbf{W}}_1) = 1$. Besides, in this case, since \mathbf{Y} is full rank, $\overline{\mathbf{W}}_E = \mathbf{0}$ according to (30). In other words, utilizing only information beam $\overline{\mathbf{w}}_1$ is optimal when $\omega_1 > 0$.

REFERENCES

- [1] Y. Chen, S. Zhang, S. Xu, and G. Li, "Fundamental Trade-offs on Green Wireless Networks," *IEEE Commun. Mag.*, vol. 49, pp. 30–37, Jun. 2011.
- [2] Z. Hasan, G. Bansal, E. Hossain, and V. Bhargava, "Energy-Efficient Power Allocation in OFDM-Based Cognitive Radio Systems: A Risk-Return Model," *IEEE Trans. Wireless Commun.*, vol. 8, pp. 6078–6088, Dec. 2009.
- [3] G. Miao, N. Himayat, and G. Li, "Energy-Efficient Link Adaptation in Frequency-Selective Channels," *IEEE Trans. Commun.*, vol. 58, pp. 545–554, Feb. 2010.
- [4] D. Ng, E. Lo, and R. Schober, "Energy-Efficient Resource Allocation in OFDMA Systems with Hybrid Energy Harvesting Base Station," *IEEE Trans. Wireless Commun.*, vol. 12, pp. 3412–3427, Jul. 2013.
- [5] I. Krikidis, S. Timotheou, S. Nikolaou, G. Zheng, D. W. K. Ng, and R. Schober, "Simultaneous Wireless Information and Power Transfer in Modern Communication Systems," *IEEE Commun. Mag.*, vol. 52, no. 11, pp. 104–110, Nov. 2014.
- [6] S. Bi, C. Ho, and R. Zhang, "Wireless Powered Communication: Opportunities and Challenges," *IEEE Commun. Mag.*, vol. 53, pp. 117–125, Apr. 2015.
- [7] X. Chen, Z. Zhang, H.-H. Chen, and H. Zhang, "Enhancing Wireless Information and Power Transfer by Exploiting Multi-Antenna Techniques," *IEEE Commun. Mag.*, vol. 53, pp. 133–141, Apr. 2015.
- [8] L. Varshney, "Transporting Information and Energy Simultaneously," in *Proc. IEEE Intern. Sympos. on Inf. Theory*, Jul. 2008, pp. 1612–1616.
- [9] X. Zhou, R. Zhang, and C. K. Ho, "Wireless Information and Power Transfer: Architecture Design and Rate-Energy Tradeoff," *IEEE Trans. Commun.*, vol. 61, pp. 4754–4767, Nov. 2013.
- [10] E. Boshkovska, D. Ng, N. Zlatanov, and R. Schober, "Practical Non-linear Energy Harvesting Model and Resource Allocation for SWIPT Systems," *IEEE Commun. Lett.*, vol. PP, no. 99, 2015.
- [11] R. Zhang and C. K. Ho, "MIMO Broadcasting for Simultaneous Wireless Information and Power Transfer," *IEEE Trans. Wireless Commun.*, vol. 12, pp. 1989–2001, May 2013.
- [12] D. W. K. Ng, E. S. Lo, and R. Schober, "Wireless Information and Power Transfer: Energy Efficiency Optimization in OFDMA Systems," *IEEE Trans. Wireless Commun.*, vol. 12, pp. 6352–6370, Dec. 2013.
- [13] X. Chen, X. Wang, and X. Chen, "Energy-Efficient Optimization for Wireless Information and Power Transfer in Large-Scale MIMO Systems Employing Energy Beamforming," *IEEE Wireless Commun. Lett.*, vol. 2, pp. 667–670, Dec. 2013.
- [14] N. Vucic and H. Boche, "Robust QoS-Constrained Optimization of Downlink Multiuser MISO Systems," *IEEE Trans. Signal Process.*, vol. 57, pp. 714–725, Feb. 2009.
- [15] D. W. K. Ng, E. S. Lo, and R. Schober, "Robust Beamforming for Secure Communication in Systems with Wireless Information and Power Transfer," *IEEE Trans. Wireless Commun.*, no. 8, pp. 4599–4615, Aug. 2014.
- [16] —, "Multi-Objective Resource Allocation for Secure Communication in Cognitive Radio Networks with Wireless Information and Power Transfer," *IEEE Trans. Veh. Technol.*, vol. PP, no. 99, 2015.
- [17] S. Boyd and L. Vandenberghe, *Convex Optimization*. Cambridge University Press, 2004.
- [18] M. Grant and S. Boyd, "CVX: Matlab software for disciplined convex programming, version 2.0 beta," [Online] <https://cvxr.com/cvx>, Sep. 2012.
- [19] M. Imran, E. Khatranaras, G. Auer, O. Blume, V. Giannini, Y. J. I. Godor, M. Olsson, D. Sabella, P. Skillermark, and W. Wajda, "Energy Efficiency Analysis of The Reference Systems, Areas Of Improvements and Target Breakdown," *EARTH Project Deliverable D*, vol. 2, Jun. 2011.